Clays and Clay Minerals, Vol. 56, No. 1, 49–65, 2008.

THE VISCOSITY OF ORGANIC LIQUID SUSPENSIONS OF TRIMETHYLDOCOCYLAMMONIUM-MONTMORILLONITE COMPLEXES

MAKOTO MINASE[1,2], MITSUJI KONDO[1], MASANOBU ONIKATA[1], AND KATSUYUKI KAWAMURA[2]

[1] Laboratory of Applied Clay Technology (LACT), Hojun Co. Ltd., 1433-1 Haraichi, Annaka, Gunma 379-0133, Japan
[2] Department of Earth and Planetary Sciences, Tokyo Institute of Technology, 2-12-1 Ookayama, Meguro-ku, Tokyo 152-8551, Japan

Abstract—An organophilic bentonite was prepared by means of a reaction of natural Na-montmorillonite with trimethyldococylammonium which has an especially long *n*-alkyl chain. The addition of trimethyldococylammonium to montmorillonite was in the range 0.25−3.0 times the cation exchange capacity (CEC) of the clay (*i.e.* 0.23−2.82 mmol/g clay). The particle morphology in organic liquid suspensions of organoclay complexes was studied by measuring the viscosity based on Eyring's rate process and Robinson's relative sediment volume. In toluene, montmorillonite with 1.17 mmol/g clay trimethyldococylammonium (1.25 times the CEC) had the largest specific gel volume, relative sediment volume, and *K*-factor. The results of the stoichiometry for trimethyldococylammonium-montmorillonite show that practically all of the quaternary ammonium was adsorbed to montmorillonite. Maximum half widths of 001 reflections from X-ray diffraction patterns were obtained in the range 0.74−1.17 mmol/g clay, indicating a disordered arrangement of the organic cation molecules intercalated between the layers. Appreciable shifts to lower-frequency regions in the Fourier transform infrared absorption spectra as a result of CH_2-stretching vibrations were observed with increasing amounts of the organic cation. When increasing the amount of organic cation added to the clay from 0.94 to 1.41 mmol/g clay, a large shift occurred to the lower-frequency side, approaching the frequency of the organic cation alone. This indicates that the interaction between adjacent hydrocarbon chains becomes progressively stronger, due to van der Waals attraction, with increases in the amount of organic cation. Interactions of the alkyl chains in trimethyldococylammonium-montmorillonite complexes with irregularly distributed and randomly arranged alkyl chains between the silicate layers were weak, and, as a result, solvation with external organic liquids occurred and gel formation developed through macroscopic swelling of the organoclay.

Key Words—FTIR Absorption Spectra, Organophilic Bentonite, Particle Morphology, Relative Sediment Volume, Specific Gel Volume, Specific Plastic Viscosity, Stoichiometry, Structure, Trimethyldococylammonium, XRD 00*l* Reflection.

INTRODUCTION

Hauser in 1938 (and published in 1950) discovered that certain organic ammonium complexes of montmorillonite, based on cation exchange, have the ability to solvate, swell, and disperse in organic liquids. The organophilic characteristics of various aliphatic ammonium-montmorillonite complexes in organic liquids were investigated by Jordan (1949) and Jordan *et al*. (1950). These organic ammonium-montmorillonite complexes have been referred to as 'organophilic bentonite' and used industrially as thickeners or reinforcing fillers for lubricating grease, paint, printing ink, plastics, *etc.* (Jordan, 1961). Organophilic bentonite has also been used as a rheological additive in various industries. The unique feature in these organic ammonium compounds is the existence of exclusively octadecyl groups, consisting of 18 carbon atoms, as long alkyl groups on trimethyloctadecylammonium, dimethyldioctadecylammonium, or dimethyloctadecylbenzylammonium.The methods for evaluating its solvation and dispersing capabilities in organic liquids have relied predominantly on measurements of swelling power and viscosity.

Recently, structural studies on organophilic bentonites and/or organic ammonium smectite complexes have been continued by other investigators with interesting results. Much information on the structure of organo-montmorillonite complexes has been provided by using infrared (IR) spectroscopy, thermal analysis, and electron microscopy (EM), as well as X-ray diffraction (XRD). The structures of organo-montmorillonite complexes have been suggested to be interstratified (Brown, 1961). Octadecylammonium-montmorillonite complexes give increased interlayer spacings with increasing organic content (Jordan *et al.*, 1950; Suito *et al*., 1966a, 1966b). The layer structure of these organoclays was also studied by EM and selected area electron diffraction. The observed lattice spacings of the image were 6.6, 4.5, 4.4, 4.0, 2.7, 2.5, and 1.8 nm. Dislocations were often seen in the lattice image and the spacings were sometimes locally different, even within a single particle. These results show the disorder of the interlayer structure of organo-montmorillonite layers (Suito *et al*., 1969; Suito

* E-mail address of corresponding author:
minase@hojun.co.jp
DOI: 10.1346/CCMN.2008.0560105

and Yoshida, 1971). Recently, similar results of irregular wavy layer structures with various *d* values on hexadecyltrimethylammonium-smectite were revealed by direct observation using EM (Lee and Kim, 2002).

The formation of monolayers (basal spacing: 1.34−1.36 nm), bilayers (basal spacing: 1.77 nm), pseudotrimolecular layers (basal spacing: ≈2.17 nm), and paraffin-like arrangements of alkylammonium ions in the interlayer spaces of *n*-alkylammonium-montmorillonites was investigated by means of the charge density of the clay (Lagaly and Weiss, 1969, 1970; Lagaly *et al*., 1976), and the monolayer, bilayer, and monolayer interstratification, and bilayer configurations of hexadecyltrimethylammonium cations in the interlayer spaces of montmorillonite were discussed by Bonczek *et al*. (2002).

They found that intercalated chains in *n*-alkylammonium smectites exist in states with varying degrees of order, because, as the interlayer packing density or the chain length decreases or the temperature increases, the intercalated chains adopt a more disordered, liquid-like structure resulting from an increase in the *gauche/trans* conformer ratio (Vaia *et al*., 1994). The ordering of conformation depends heavily on hexadecylamine concentration and orientation. The chains adopt an essentially all-*trans* conformation with orientation radiating away from the silicate surface when the amine concentration is large. On the other hand, a disordered *gauche* conformer is introduced to the chain when amine chains have orientations parallel to the silicate layers, with the amount of *gauche* conformer increasing as amine concentration decreases (Li and Ishida, 2003). In addition to results from FTIR spectroscopy and thermal analysis, study by means of nuclear magnetic resonance on the fine structure of hexadecyltrimethylammonium molecules intercalated in the interlayer of montmorillonite demonstrated the coexistence of the ordered (all-*trans*) and disordered (mixture of *trans* and *gauche*) conformations, depending on the condition of their orientation and packing density within the interlayer (He *et al*., 2004).

Hexadecylammonium molecules intercalated between smectite layers form flat-lying monolayers (layer spacing: 1.36 nm), flat-lying bilayers (layer spacing: 1.76 nm), and tilted paraffin-like arrangements (2.65 nm) or interstratifications of these. Uptake of neat toluene occurs only for hexadecylammonium intercalates with bilayer and paraffin-like interlayer arrangements, which give d_{001} values of between 3.3 and 4.5 nm (Slade and Gates, 2004a). Studies of hexadecyltrimethylammonium-vermiculites indicated that, in liquid toluene, the extent of interlayer swelling is sufficient to overcome the interdigitation, and disorder in the interlayer occupancy by the organic cation occurs (Slade and Gates, 2004b).

The flow behavior of bentonite colloidal suspensions in water, glycerol, and oil (organophilic bentonite) was given in terms of the stress-strain (shear stress-shear rate) relations, based on Eyring's rate theory of viscosity (Powell and Eyring, 1944), with respect to variables of concentration, suspension medium, pH, electrolyte concentration, temperature, and the successive application of shear stress (Gabrysh *et al*., 1963). Flow curves, as a general rule, will give an up-curve by increasing the shear rate, and a down-curve by decreasing the rate in the reverse direction, or both. Cycling of up-curve and down-curve produces thixotropic hysteresis loops. Frequently, in a flow system two kinds of units are found, entangled and disentangled. The entangled units first exhibit non-Newtonian flow properties and then transform to the disentangled units of Newtonian character as a result of shear. If the stress is relieved, the transformed unit tends to return to its original state. This change in equilibrium conditions can be represented by the following: entangled ⇌ disentangled. Thus, two types of dispersed particles should be considered. Type 2 acts as a Newtonian unit and type 1 as a non-Newtonian unit (Gabrysh *et al*., 1963; Park *et al*., 1971; Low, 1992). These studies were accomplished by focusing in particular on the type 1 units, or the study of the bulge at low shear rate.

For the viscosity of Newtonian flow of a suspension, the Einstein equation (1906) is based on certain necessary assumptions, the main ones being that the suspended particles are rigid spheres and that their concentration is so small that no interactions occur among the particles (Green, 1949). Subsequently, the Einstein equation was modified by introducing the concept of intrinsic viscosity and particle morphology (Kuhn and Kuhn, 1945), the volume of free liquid and relative sediment volume in a suspension (Robinson, 1949), and a critical-volume concentration of suspended particles (Mori and Ototake, 1956).

In a previous study (Minase *et al*., 2006), we analyzed the effects of aqueous suspension concentration and swelling characteristics of commercially available bentonite samples on their flow behavior. We also investigated the micro-morphology of the bentonite particles as flow units in the clay aqueous suspension. The interrelation of the liquid limit, the swelling power, and the flow unit were considered by applying the concept of Atterberg limits of soils as a function of water content (Grim, 1962; Mitchell and Soga, 2005).

Current work is directed toward the dococyl groups consisting of 22 carbon atoms with longer hydrocarbon-chain lengths derived from erucic acid, a fatty acid of rapeseed oil, and trimethyldococylammonium-montmorillonite (TMDCA-Mt) complexes. The viscosity of the non-polar organic liquid suspensions of these organoclay complexes was measured and the organoclay particle morphology in the high-concentration suspensions was investigated by deducing the rheological concept on the intrinsic viscosity (*k*-factor) as a function of the aspect ratio of particles, the relative sediment

Table 1. General properties of the initial clay.

Moisture (wt.%)	Swelling power* (cm^3/2 g)	Specific gel volume of water, f_{aq}** (cm^3/cm^3)	Density (g/cm^3 at 25ºC)	Methylene blue absorption (mmol/100 g)	Cation exchange capacity (meq/100 g)
8.08	41.5	53.9	2.60	115	94

Chemical analysis (wt.%)									
SiO_2	TiO_2	Al_2O_3	Fe_2O_3	MgO	CaO	Na_2O	K_2O	Loss on ignition	Total
59.98	0.12	21.82	3.52	2.90	0.86	2.79	0.31	6.86	99.16

* U.S. Pharmacopoeia, Bentonite, swelling power
** suggesting swelling capacity per unit volume of clay

volume, and the critical-volume concentration described above (Kuhn and Kuhn, 1945; Robinson, 1949; Mori and Ototake, 1956). In addition, the formation of TMDCA-Mt complexes and the structure of the organoclay complexes were investigated, based on stoichiometry, with differential thermogravimetric analysis (DTGA), and structural analysis with powder XRD and Fourier transform infrared (FTIR) spectroscopy. The relationship between the structure and the organophilicity of the organoclay complexes prepared in the present study will be discussed in the context of order-disorder in the organization of intercalated organic cations between the silicate layers.

MATERIALS AND METHODS

Montmorillonite

The clay used in these experiments was natural Na-montmorillonite separated from bentonite from Colony, Wyoming. The preparation was as follows. The bentonite was suspended in deionized water; after standing overnight, the suspension was decanted to eliminate non-clay sediment, then the <1.0 μm fraction was extracted by centrifugation. The clay was essentially pure montmorillonite according to thermal and XRD analysis. A brief description of the initial clay is given in Table 1.

Trimethyldococylammonium chloride

A commercially available trimethyldococylammonium chloride (TMDCA-Cl) was used as received to prepare the organoclay complexes. The chemical characteristics are listed in Table 2.

Table 2. Chemical characteristics of trimethyldococylammonium chloride*.

Chemical formula	Formula weight	Concentration (wt.%)
$C_{22}H_{45}N^+(CH_3)_3{\cdot}Cl^-$	403.5	80.4

* Trade name: ARQUAD 22-80, supplied by Lion Akuzo

Non-polar organic liquid

A commercially available naphthene-base process oil (NPO), which is used as a petroleum softener for rubber, was used as the suspension medium because it is widely regarded as exhibiting no volatile loss when used in the preparation of suspensions and the determination of viscosity. Its general properties are listed in Table 3.

Preparation of TMDCA-Cl aqueous solution. The 10 wt.% TMDCA-Cl aqueous solution with deionized water was prepared in a beaker. The solution became colorless, transparent, and thin by heating at 50ºC. We checked for possible adhesion of some of the TMDCA-Cl to the beaker wall by weighing the beaker emptied of its contents, but no appreciable change in the weight was noted.

Preparation of TMDCA-Mt complexes

The 2 wt.% clay-deionized water suspensions were prepared and heated to 50ºC. The 10 wt.% TMDCA-Cl aqueous solution at 50ºC was added to the clay suspension under vigorous stirring. After 2 h the precipitates were filtered, and washed with deionized water several times until the chloride ion concentration in the filtrate was <~8 ppm by titrating with $AgNO_3$. The cakes were then dried in an oven with circulating air at 85ºC and pulverized in a laboratory hammer mill. The ratio of the TMDCA-Cl to the clay was in the range of 0.25–3.0 times the CEC of the clay (*i.e.* 0.23–2.82 mmol/g clay).

Preparation of organoclay-organic liquid suspensions

First, a 7 wt.% pre-gel of organoclay-organic liquid was prepared. The procedure was as follows: 54 g of the organoclay were added to 68 g of NPO and stirred with a high-speed disk mixer for 20 min; then 18.5 g of an aqueous methanol solution (95 wt.% methanol, 5 wt.% water), used as a gelling accelerator, were added to this batch under continuous stirring, and heated to 60ºC, followed by further stirring for 10 min. The batch was then allowed to stand for 24 h. After preparation of the pre-gel, organoclay-NPO suspensions of various concentrations were prepared for the viscosity measurements by diluting this pre-gel with an additional NPO in

https://doi.org/10.1346/CCMN.2008.0560105 Published online by Cambridge University Press

Table 3. General properties of naphthene base process oil*.

Density (g/cm^3 at 25ºC)	Kinematic viscosity (mm^2/s at 98.9ºC)	Flash point (ºC)	Refractive index	Pour point (ºC)	Aniline point (ºC)
0.9230	3.686	162	1.5114	−47.5	62.0

* Trade name: SYNTAC N-65, supplied by Kobe Oil Chemical Industrial Co., Ltd.

the high-speed impeller mixer (Hamilton Beach Mixer, 11000±300 rpm) specified by American Petroleum Institute Standard (API Spec. 13A) for 20 min at 25±0.5ºC. Each suspension was allowed to stand for 30 min, then stirred again for 1 min in the mixer. The viscosity of the suspensions was measured immediately. For comparison, the NPO suspension of a commercially available organophilic bentonite and the aqueous suspension of the initial clay were prepared and the viscosity was measured.

Method for measuring the viscosity and flow curve

The top shear rate of 500, 700, or 1020 s^{-1} can be found on the flow curve of bentonite or from the previously reported organophilic bentonite suspension (Gabrysh *et al*., 1963; Park *et al*., 1971; Low, 1992; Minase *et al*., 2006). The method used in the present study is described below.

The apparatus used to measure viscosity and flow parameters was the direct-indicating rotational viscometer (Fann V-G Meter Model 35A, specified API Spec. 13A). Each of the flow curves (*i.e*. down-curves, Green, 1949) was determined by plotting shear stress (τ, Pa) as a function of shear rate (σ, s^{-1}) for decreasing shear rates. Extrapolated yield stress (τ_e, Pa) was obtained from the intercept, which was established by extrapolating the straight part of down-curve to the shear-stress axis, provided that the critical shear rate, σ_c, was 510 s^{-1} according to the API examination method for bentonite mud. Extrapolated yield stress and plastic viscosity (η_{pl}, Pa s) were obtained from the following equations (Güven, 1992a):

$$\tau_e = 2\tau_{510} - \tau_{1020} \quad (1)$$

$$\eta_{pl} = (\tau_{1020} - \tau_e)/\sigma_{1020} \quad (2)$$

where subscripts '510' and '1020' mean the shear rate, s^{-1}.

Miscellaneous examinations

The density of the organoclay samples was determined pycnometrically with kerosene at 25ºC in order to discover the volume of the organoclay particles in organic liquids. In order to assess the effectiveness of the organic cation molecules in converting the initial clay to the organophilic condition, the apparent gel volume of 0.5 g of each of the pulverized organoclay samples in 25 mL of toluene was measured by applying the method derived by Jordan (1949). The volume was then converted to a specific gel volume of toluene, f_t (cm^3/cm^3), based on the unit volume of the organoclay particles. In addition, stoichiometrical and structural information for TMDCA-Mt complex formation was obtained by means of DTGA, XRD, and FTIR. The FTIR data were obtained using the diffuse reflectance (DR) method and the CCl_4-mull method. The following equipment was used: DTGA: Rigaku Corporation, Thermo Plus 2TG-DTA TG8120; XRD: Rigaku Corporation, RAD-IIA, Cu X-ray tube voltage of 25 kV, tube current of 15 mA; FTIR, DR method: Jasco Corporation, FT/IR-6100; and CCl_4-mull method: the Perkin-Elmer Corporation, Paragon 1000 FTIR.

RESULTS AND DISCUSSION

Brief descriptions of nine TMDCA-Mt complexes are given in Table 4. Of these, the complex formed from 1.17 mmol/g clay, which corresponds to 1.25 times the CEC value, has the largest specific gel volume of toluene, f_t.

Flow behavior

Rheogram determinations of the organoclay-NPO suspensions were determined for the four TMDCA-Mt complexes of 0.94, 1.17, 1.41, and 1.88 mmol/g clay (*i.e*.

Table 4. Description of TMDCA-Mt complexes produced in the present experiments.

Amount of organic cation added, *a*:									
(mmol/g clay)	0.23	0.47	0.70	0.94	1.17	1.41	1.88	2.35	2.82
CEC	0.25	0.50	0.75	1.00	1.25	1.50	2.00	2.50	3.00
Density (g/cm^3)	1.9508	1.8441	1.7607	1.7004	1.5692	1.5466	1.4579	1.3431	1.3007
Specific gel volume of toluene, f_t (cm^3/cm^3)	3.1	3.3	8.1	38.1	45.3	29.3	21.9	20.7	19.5

https://doi.org/10.1346/CCMN.2008.0560105 Published online by Cambridge University Press

1.00, 1.25, 1.50, and 2.00 CEC, respectively), having substantial f_t values (see Table 4). The down-curves are shown in Figure 1. Each curve exhibits plastic flow according to equation 3 (Güven, 1992a).

$$\tau = \eta_{pl} \cdot \sigma + \theta \tag{3}$$

where θ is yield stress. Extending the Einstein (1906) equation to higher concentrations, Robinson (1949) introduced the concept that the specific viscosity is not only proportional to the volume fraction of the suspended fine solid particles, but is also inversely proportional to the volume of the free liquid in the suspension. He then proposed equation 4 based on experimental results from the suspensions of glass spheres of 10–20 μm in various liquids, showing Newtonian flow within the range of the solid-volume fraction of ~0.10–0.5.

$$\frac{\eta - \eta_0}{\eta_0} = \eta_r - 1 = \eta_{sp} = k \times \frac{\phi}{(1 - S'\phi)} \tag{4}$$

where η is the viscosity of the suspension; η_0 is the viscosity of the solvent; η_r is the relative viscosity; η_{sp} is the specific viscosity; k is a factor which is the intrinsic viscosity by definition, representing the specific contribution of a solid particle to the viscosity of a suspension and the minimum k value of 2.5 is considered a constant (the Einstein constant) when the solid is a rigid sphere; ϕ is the volume fraction of the suspended solid; and S' is the relative sediment volume. Therefore the sediment volume in the unit volume of the suspension is $S'\phi$ and the volume of the free liquid is $1-S'\phi$.

Following a suggestion by Robinson (1949), Mori and Ototake (1956) assumed that the thickness of the liquid phase responsible for shearing deformation is measured normal to the direction of shear of the liquid layer between adjacent particles. Basing their arguments on Bingham's (1922) observation, which states that all particles in a shearing liquid experience the same velocity and that the distances between particles is constant, they deduced the shear stress and viscosity equations (equations 5 and 6). These equations clarified the physical meaning of the Robinson equation (equation 4). Further, Mori and Ototake (1956) proposed that a critical volume fraction, ϕ_c, exists, which is the solid volume at which particle deformation under constant shear stress no longer occurs.

$$\tau = \eta_0 \cdot \frac{\Delta u}{\delta} = \eta \cdot \frac{\Delta u}{D + \delta},\ \delta = \frac{2}{s_0} \cdot \left(\frac{m_s}{\rho_s}\right)\left(\frac{1}{\phi} - \frac{1}{\phi_c}\right) \tag{5}$$

$$\eta_{sp} = \frac{D}{2} \cdot \frac{s_0}{(m_s/\rho_s)} \cdot \frac{1}{(1/\phi) - (1/\phi_c)} = \frac{D}{2} \cdot \frac{s_0}{(m_s/\rho_s)} \cdot \frac{\phi}{(1 - S'\phi)} \tag{6}$$

where τ is the shear stress, Δu is the difference in the velocity of flow, δ is the thickness of the liquid between adjacent particles in the normal direction of shearing, D is the average particle size of the suspended solid, s_0 is the total surface area of the particles existing in the system, m_s is the total mass of the particles in the system, ρ_s is density of the solid, and ϕ_c is the maximum solid-volume fraction (*i.e.* where the solid particles in the suspension can be deformed continuously and stably by shearing, the critical-volume fraction mentioned above; see Figure 2).

One of the goals of the present study was to obtain some information on the morphological features of the flow units on the organoclay-organic liquid suspensions at medium or high solid concentration. However, the viscosity of the suspensions varies with the shear rate because flow type is non-Newtonian. Therefore, we considered that the Robinson equation for the Newtonian fluid could not simply be applied to the plastic fluids illustrated in Figure 3.

According to Powell and Eyring (1944), a solid-liquid suspension that displays plastic flow involves the

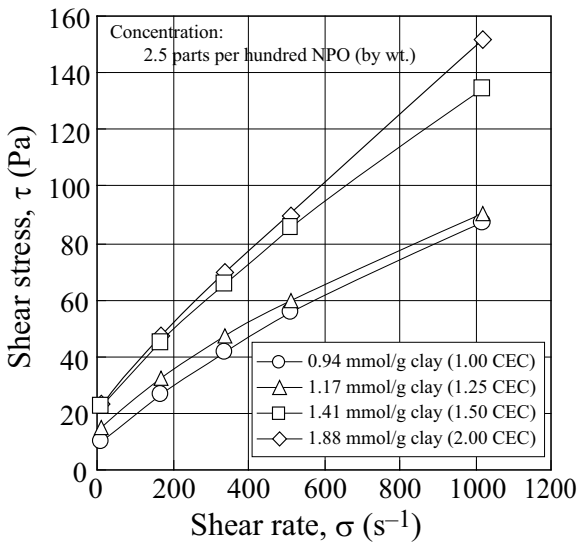

Figure 1. Relationship between shear stress, τ, and shear rate, σ, for suspensions of the four organoclays at a concentration of 2.5 parts per hundred NPO (by wt.).

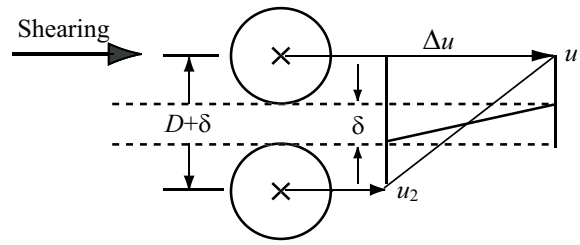

Figure 2. Schematic diagram of suspended particles sheared at high concentration, proposed by Mori and Ototake for the Robinson equation.

https://doi.org/10.1346/CCMN.2008.0560105 Published online by Cambridge University Press

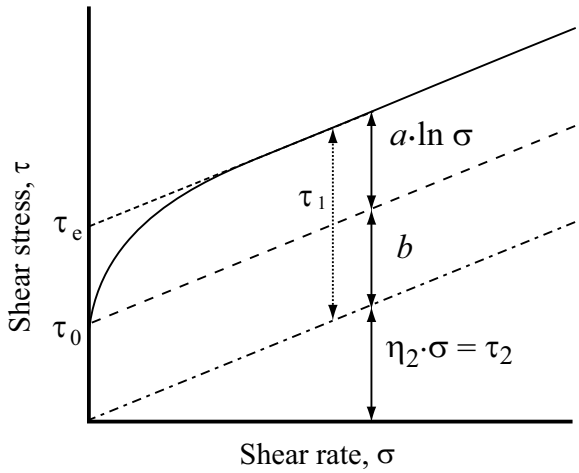

Figure 3. Schematically interpretative diagram of the relationship between equations 7 and 8 in plastic flow.

breaking of at least two types of bonds. Type 1 consists of strong bonds exhibiting flow described by non-Newtonian law (at moderate stress, exponential law), while type 2, comprising weak bonds, obeys the Newtonian law (*i.e.* flow is proportional to stress). The total stress, τ, is expressible as a sum by equation 7

$$\tau = \tau_1 + \tau_2 \tag{7}$$

where τ_1 is the shear stress acting on the type-1 bonds and τ_2 on type-2 bonds. They found that the plastic flow curve of lubricating grease can be expressed by equation 8 according to the rate process of Eyring

$$\tau = \eta_2 \cdot \sigma + a \cdot \ln\sigma + b \tag{8}$$

where a and b are constants, the $\eta_2 \cdot \sigma$ term is the type-2 bonds, the $a \cdot \ln \sigma$ term is part of the shear stress due to the type-1 bonds depending on the shear rate, and b is the shear stress at zero shear rate. The first term in equation 8 represents the Newtonian component, which is determined by hydrodynamic effects, and both the second term and the b constant are ascribable to the effects of particle interaction. The experimental flow curves on montmorillonite-water suspensions of medium to high concentration and organophilic bentonite grease were described comprehensively by Gabrysh *et al.* (1963), Park *et al.* (1971), and Low (1992) in terms of Eyring's rate theory and the general viscosity equation. The correlation of equations 7 and 8 for plastic flow behavior is illustrated schematically in Figure 3, thereby the above equations can be be expressed concisely as equation 9.

$$\tau = \eta_{pl} \cdot \sigma + \tau_e \tag{9}$$

where η_{pl} is the plastic viscosity of the suspension and τ_e is the extrapolated shear stress (*i.e.* the extrapolated yield stress).

The specific plastic viscosity of the suspension, $\eta_{sp/pl}$, is thus proportional to the increase in the plastic viscosity of the suspension, η_{pl}, over that of the suspending medium (*i.e.* solvent), η_0, by equation 10, because the $\eta_{pl} \cdot \sigma$ term equals the Newtonian term, as mentioned above.

$$\eta_{sp/pl} = \frac{\eta_{pl} - \eta_0}{\eta_0} \tag{10}$$

By substituting the $\eta_{sp/pl}$ for η_{sp} in the original Robinson equation (equation 4), the k factor and the relative sediment volume, S', of the organoclay particles flow units can be obtained by means of equations 11, 12, and 13.

$$\eta_{sp/pl} = k \times \frac{\phi}{(1 - S'\phi)} \tag{11}$$

$$\frac{1}{\eta_{sp/pl}} = \frac{1}{k} \cdot \frac{1}{\phi} - \frac{S'}{k} = \frac{1}{k}\left(\frac{1}{\phi} - S'\right) \tag{12}$$

$$1 - S'\phi_c = 0, \quad \phi_c = \frac{1}{S'} \tag{13}$$

where ϕ is the volume fraction and ϕ_c is the critical-volume fraction of the organoclay particles. The latter is indicative of the concentration where free liquid no longer exists and a precipitous increase in plastic viscosity of the suspension occurs due to particle interaction.

The viscosity determinations were interpreted according to the theoretical background mentioned above, and the experimental results are given in Table 5 and in Figure 4(a–d). The reciprocal specific plastic viscosity, $1/\eta_{sp/pl}$, is plotted as a function of the reciprocal volume fraction, $1/\phi$, in Figure 4a–d. All of the NPO suspensions of the four organoclays show an excellent, straight-line regression. The relative sediment volume, S', the k factor (*i.e.* intrinsic viscosity), the aspect ratio (*i.e.* *a/c* for an oblate ellipsoid: Kuhn and Kuhn, 1945; Güven, 1992b), and the critical-volume fraction, ϕ_c, are given in the right-most column of Table 5. The value of relative sediment volume, S', obtained during the current investigation can be considered to be a dynamic swelling capacity per unit volume of the organoclay particles, with the greatest magnitude obtained with the TMDCA addition of 1.17 mmol/g clay.

In previous investigations, the magnitute of k factor values of ~100–200 were proposed for aqueous suspensions for Na-montmorillonite particles (Egashira, 1977; Onikata and Kondo, 1995). As shown in Table 5, the k-factor value and the aspect ratio of the initial montmorillonite particles, used in the present study, in aqueous suspension, were 174 and 254, respectively. However, the k-factor values and the aspect ratios of all of the organoclay particles (containing TMDCA-Mt complexes and Bentone 34®) in the NPO suspensions tested in this investigation were ~10–17 and 14–23,

https://doi.org/10.1346/CCMN.2008.0560105 Published online by Cambridge University Press

Table 5. Rheological data on NPO suspensions of organoclay complexes and aqueous suspensions of the initial clay.

Samples	Items	Concentrations of organoclay (parts per hundred NPO, by wt.) 1.0	1.5	2.0	2.5	3.0	3.5	Robinson's parameters and aspect ratio
TMDCA-1.00, 0.94 mmol/g clay								
	$1/\phi$	–	124	93.2	74.8	62.5	53.7	S': 41.2
	η_{pl} (mPa s)	–	52.6	56.5	61.2	75.4	89.0	k-factor: 11.7
	$1/\eta_{sp/pl}$	–	6.786	4.302	2.986	1.551	10.62	Aspect ratio: 16
	τ_e (Pa)	–	9.24	14.8	24.2	27.4	36.2	ϕ_c: 0.0243:
TMDCA-1.25, 1.17 mmol/g clay								
	$1/\phi$	171	114	86.0	69.0	–	–	S': 62.6
	η_{pl} (mPa s)	52.4	59.3	86.2	122	–	–	k-factor: 16.1
	$1/\eta_{sp/pl}$	6.725	3.334	1.124	0.600	–	–	Aspect ratio: 22
	τ_e (Pa)	7.72	18.9	26.9	27.7	–	–	ϕ_c: 0.0160
TMDCA-1.50, 1.41 mmol/g clay								
	$1/\phi$	169	113	84.8	68.0	–	–	S': 55.5
	η_{pl} (mPa s)	52.4	57.9	77.5	96.4	–	–	k-factor: 16.5
	$1/\eta_{sp/pl}$	6.775	3.714	1.431	0.898	–	–	Aspect ratio: 23
	τ_e (Pa)	6.37	17.5	28.8	35.8	–	–	ϕ_c: 0.0180
TMDCA-2.00, 1.88 mmol/g clay								
	$1/\phi$	–	106	–	64.2	53.7	46.2	S': 30.0
	η_{pl} (mPa s)	–	52.0	–	60.0	69.5	71.3	k-factor: 10.7
	$1/\eta_{sp/pl}$	–	7.146	–	3.172	1.910	1.776	Aspect ratio: 14
	τ_e (Pa)	–	7.82	–	29.1	37.1	58.3	ϕ_c: 0.0333
Bentone-34* (control)								
	$1/\phi$	161	108	81.0	65.0	–	–	S': 53.4
	η_{pl} (mPa s)	45.4	47.7	58.8	73.1	–	–	k-factor: 12.0
	$1/\eta_{sp/pl}$	6.391	4.650	2.009	1.160	–	–	Aspect ratio: 16
	τ_e (Pa)	3.14	8.70	24.0	52.3	–	–	ϕ_c: 0.0187

	Concentrations of the original montmorillonite (parts per hundred water, by wt.) 2.0	3.0	4.0	5.0	
The initial montmorillonite control					
$1/\phi$	134	90.0	67.8	54.5	S': 46.3
η_{pl} (mPa s)	2.6	5.1	8.7	12.8	k-factor: 174
$1/\eta_{sp/pl}$	0.523	0.212	0.114	0.0751	Aspect ratio: 254
τ_e (Pa)	0.15	0.46	1.43	4.19	ϕ_c: 0.0216

* Dimethyldioctadecylammonium-montmorillonite, produced by RHEOX, Inc.

respectively, one order less than those of the initial montmorillonites in aqueous suspension. Here the k factor and the aspect ratio as oblate ellipsoids were calculated according to the approximation of Kuhn and Kuhn (Güven, 1992b).

Stoichiometry of TMDCA-Mt complex formation

The thermal reactions of montmorillonite summarized by Grim (1968), and Brindley and Lemaitre (1987), are given in Table 6. The use of DTGA with ignition in the oxidizing atmosphere is expected to allow different types of

Table 6. Summary of the thermal reaction of montmorillonite.

Low-temperature reactions	Intermediate-temperature reactions		High-temperature reactions	
Montmorillonite* $\rightarrow$150–250ºC	$\rightarrow$ Montmorillonite anhydride $\rightarrow$ 700ºC	Montmorillonite dehydroxylate 1000ºC $\rightarrow$	Spinel-type phase with cryptocrystalline quartz 1150ºC	Mullite with cristobalite

* Ideal formula $M^{+}_{1/3}nH_2O[(Al_{5/3}Mg_{1/3})Si_4O_{10}(OH)_2]^{1/3-}$

https://doi.org/10.1346/CCMN.2008.0560105 Published online by Cambridge University Press

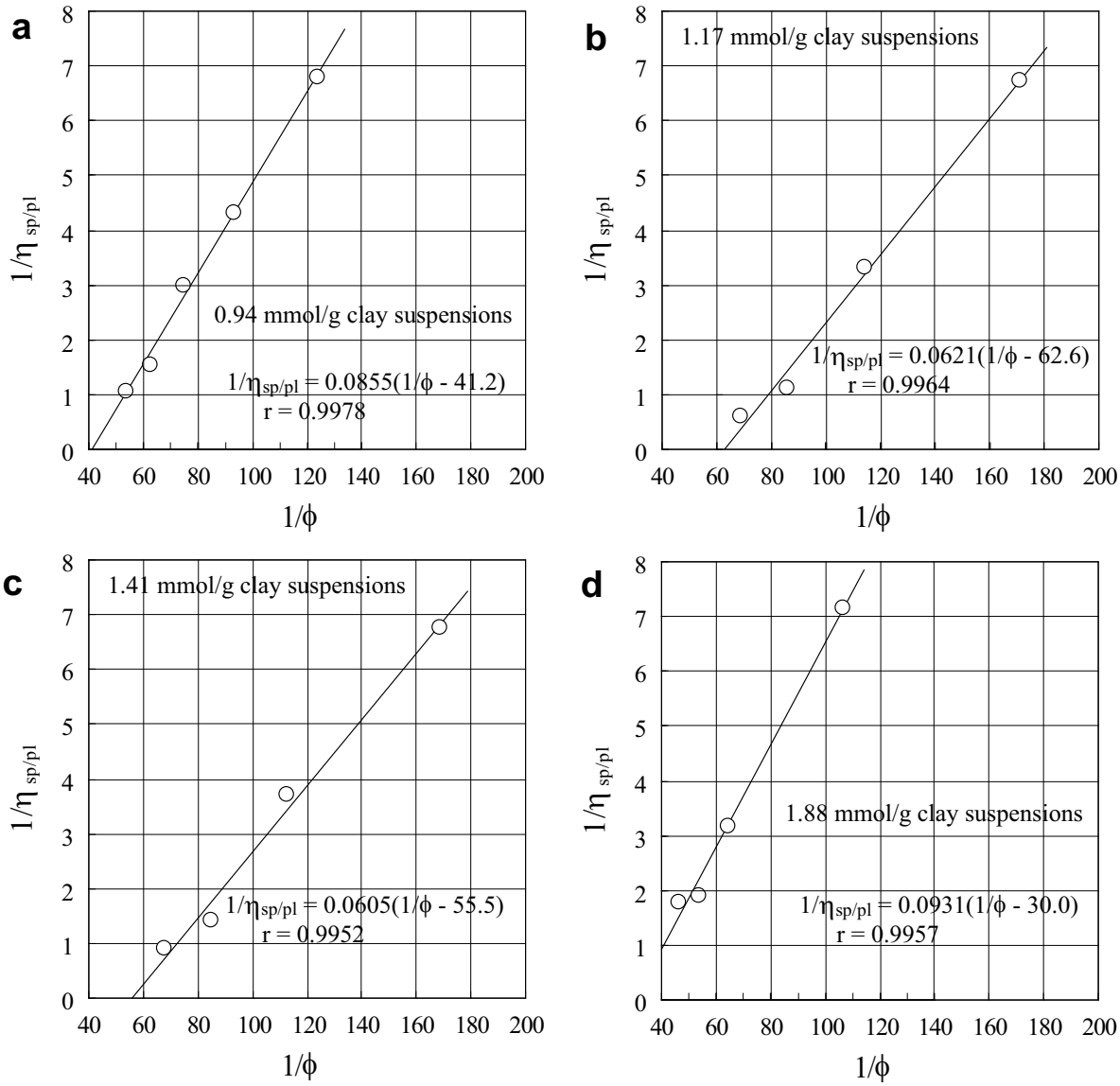

Figure 4. (a) Plot of $1/\eta_{sp/pl}$ *vs.* $1/\phi$ for suspensions of TMDCA-1.00 (0.94 mmol/g clay) organoclay in NPO. (b) Plot of $1/\eta_{sp/pl}$ *vs.* $1/\phi$ for suspensions of TMDCA-1.25 (1.17 mmol/g clay) organoclay in NPO. (c) Plot of $1/\eta_{sp/pl}$ *vs.* $1/\phi$ for suspensions of TMDCA-1.50 (1.41 mmol/g clay) organoclay in NPO. (d) Plot of $1/\eta_{sp/pl}$ *vs.* $1/\phi$ for suspensions of TMDCA-2.00 (1.88 mmol/g clay) organoclay in NPO.

mass loss in the organoclay complexes to be differentiated and the relative amounts of interlayer water (structural or hydroxyl) and organic matter to be determined. However, in practice, the temperature ranges of dehydroxylation of the clay and oxidative reaction of the organic matter overlap, and as a result, defining the separation of overlapping reactions may be difficult. The mass ratio of structural water per residue should be constant, and multiplication of the mass of the residue by a factor gives the mass of the structural water for the organoclay samples, *i.e.*:

$$[\text{mass of structural water}]/[\text{mass of residue}] = k_r \text{ (constant)} \quad (14)$$

where k_r is the mass-ratio factor.

El-Akkada *et al.* (1982) demonstrated that the exchangeable cation has little effect on the dehydroxylation temperature, or on the magnitude of the mass-loss. Bish and Duffy (1990) suggested that the mass-loss from 350ºC to the end of the TGA experiment is similar to the H_2O values reported for many montmorillonite samples. The k_r values computed from TGA data presented by Bish and Duffy (1990) are from 0.0575 to 0.0700, with the average value at 0.0655. In the present experiments, the k_r value of 0.0678 was determined from the DTGA curves of the organoclay consisting of 0.70 mmol/g clay, because the separation of the mass-loss due to dehydroxylation is well defined. Although this value, 0.0678, is larger than the loss on ignition,

https://doi.org/10.1346/CCMN.2008.0560105 Published online by Cambridge University Press

0.0645, for the initial clay, the difference, 0.0033, is considered to correspond to the amount of Na_2O lost in the ignition residue of the organoclay as shown in the expressions assumed below.

The reaction of the organoclay complex formation with Na-montmorillonite and the quaternary ammonium salt is given as:

$$Na^+_{1/3}\cdot[(Al_{5/3}Mg_{1/3})Si_4O_{10}(OH)_2]^{1/3-} + mR_4N^+\cdot Cl^- \rightarrow (R_4N^+)_{1/3}(R_4N^+\cdot Cl^-)_{m-1/3}\cdot[(Al_{5/3}Mg_{1/3})Si_4O_{10}(OH)_2]^{1/3-} + 1/3NaCl \quad (15)$$

where R_4N^+ is the quaternary alkylammonium cation.

The thermal reaction of organoclay is given as:

$$(R_4N^+)_{1/3}(R_4N^+\cdot Cl^-)_{m-1/3}\cdot[(Al_{5/3}Mg_{1/3})Si_4O_{10}(OH)_2]^{1/3-} \rightarrow \text{oxidation products of organic matter}_{(volatile)} + H_2O_{(volatile)} + [1/2(Al_2O_3)_{5/3}\cdot(MgO)_{1/3}(SiO_2)_4]_{(residue)} \quad (16)$$

Typical DTGA curves of the TMDCA-Mt produced in the present experiments are given in Figure 5. They show that the organic matter in the organoclay did not volatilize simply by ignition but was reduced through the oxidation process with complex variation of the weight, after which a constant residue weight remained. The quantity of organic matter was computed from equation 17 based on the total amount of residue and the structural water.

$$m_{org}\ (\text{wt.\%, measured}) = \frac{\Delta\Sigma - (\Delta w_1 + \Delta w_2)}{\Delta R + \Delta w_2} \times 100 \quad (17)$$

($\Delta w_2 = k_r\cdot\Delta R = 0.0678\cdot\Delta R$, here)

where m_{org} is the experimentally measured quantity (wt.%) of the organic matter, $\Delta\Sigma$ is total mass-loss, Δw_1 is the mass-loss of adsorbed water, Δw_2 is the mass-loss of dehydroxylation, and ΔR is the mass of the residue.

From equations 15 and 16, the stoichiometry of the Na-montmorillonite in the thermal reaction *via* organoclay is expressed in equation 18.

$$Na^+_{1/3}\cdot[(Al_{5/3}Mg_{1/3})Si_4O_{10}(OH)_2]^{1/3-} = [1/2(Al_2O_3)_{5/3}\cdot(MgO)_{1/3}(SiO_2)_4] + H_2O + 1/2(Na_2O)_{1/3} \quad (18)$$

where the $[1/2(Al_2O_3)_{5/3}\cdot(MgO)_{1/3}(SiO_2)_4]$ term and the $[H_2O]$ term represent the residue and the structural water, respectively, and they should be constant, and the $[1/2(Na_2O)_{1/3}]$ term is equivalent to the CEC of the initial clay. Therefore, the theoretical stoichiometry for the quantitative analysis of the organic matter in the thermal reaction is as follows.

The ratio of TMDCA-Cl added, $x \leqslant 1.0$:

$$m'_{org}\ (\text{wt.\%, theoretical}) = \frac{368\chi \times x + 31\chi \times x}{100 - 31\chi \times x} \times 100 \quad (19)$$

The ratio of TMDCA-Cl added, $x > 1.0$:

$$m'_{org}\ (\text{wt.\%, theoretical})\} = \frac{368\chi + 403.5\chi \times (x-1) + 31\chi \times (x-1)}{100 - 31\chi \times x} \times 100 \quad (20)$$

where m'_{org} is the theoretical quantity of the organic matter (wt.%), x is the equivalent ratio of the organic ammonium molecules added to the CEC of the initial clay (*e.g.* 0.75, 1.00, 1.25, *etc.*), χ is CEC expressed by eq/g clay, and each of the factors 368, 403.5, and 31 are the formula weights of the TMDCA ion, TMDCA-Cl, and 1/2 Na oxide, respectively. Thus, m_{org} (wt.%, measurement) from equation 17 in the DTGA experiments of all the organoclay samples and m'_{org} (wt.%, theoretical) from equations 19 and 20 as a function of a (amount of organic

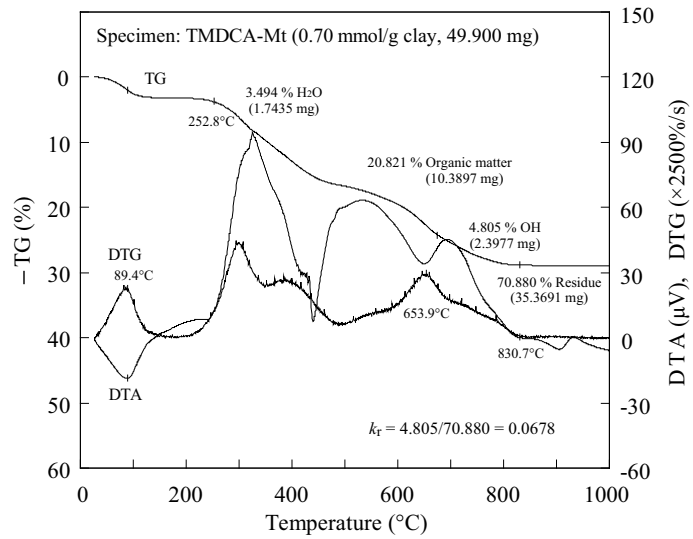

Figure 5. DTA, TG, and DTG patterns for the typical TMDCA-Mt (0.70 mmol/g clay). Atmosphere: air, rate: 10.0°C/min.

https://doi.org/10.1346/CCMN.2008.0560105 Published online by Cambridge University Press

Table 7. Quantitative data for organic matter by thermal analysis of organoclays.

Amount of organic cation added, *a*:									
(mmol/g clay)	0.23	0.47	0.70	0.94	1.17	1.41	1.88	2.35	2.82
CEC	0.25	0.50	0.75	1.00	1.25	1.50	2.00	2.50	3.00
m_{org} (wt.%, measured)	9.74	19.2	27.5	37.3	47.2	60.5	77.0	95.9	112.6
m'_{org} (wt.%, theoretical)	9.45	19.0	28.7	38.6	48.3	58.1	77.6	97.1	116.6
m_{org}/m'_{org} (%)	103.1	101.1	95.8	96.6	977.7	104.1	99.2	98.8	96.6

* Average (%): 99.2

cation added, mmol/g clay) are given in Table 7 and Figure 6. The experimental measurements correlate well with the theoretical determinations as shown in Figure 6. From this, it is determined that the organoclay complexes are produced with nearly all of the quaternary ammonium salt sorbed to the montmorillonite.

Structure of TMDCA-Mt complexes

Many investigators have given detailed descriptions, by means of XRD, of the structures of organoclay complexes produced by intercalating various alkylammonium compounds into the interlayer of the smectite structure. Jordan (1949) and Jordan *et al*. (1950) investigated the effect of the chain length, the number of the chains, and the ratio of long-chain *n*-alkyl groups ($\leqslant C_{18}$) of organic ammonium ions added on the interlayer separation of montmorillonite flakes. They proposed that the interlayer separation increased stepwise: 0.4, 0.8, 0.9−1.04, and 2.3−2.4 nm corresponding to the state where the alkylammonium molecules are adsorbed as a single layer or as double layers parallel to the basal plane, or as semi triple-layers by partially overlapping the hydrocarbon chains in the interlayer and as a single layer perpendicular to the plane, respectively. They also discovered that a minor proportion of high polar-low molecular weight organic liquid, such as methanol, increases solvation of the organophilic bentonite considerably, and provides the maximum gel volume of non-polar organic liquids. This is due to polar molecules adsorbing onto the available uncoated hydrophilic surface of the clay through the mechanism of hydrogen bonding. This adsorption renders the clay surface more completely coated with organic matter and consequently more organophilic.

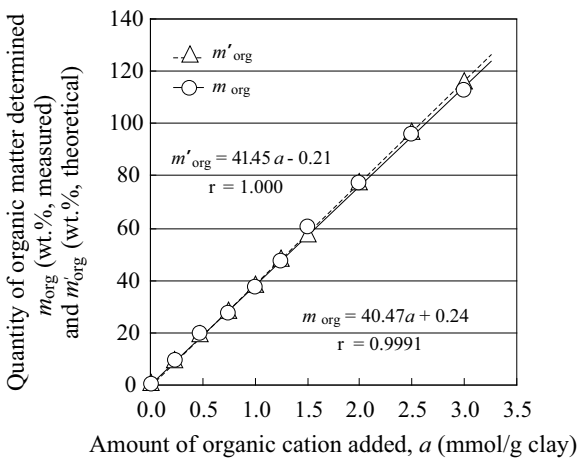

Figure 6. Plot of quantity of organic matter determined *vs*. amount of organic cation added to montmorillonite.

Figure 7a displays the raw XRD diagrams of the 00*l* reflection for the initial clay and the samples of TMDCA-Mt complexes produced in the present work. These diagrams illustrate changes due to the increasing amount of organic cations added to montmorillonite. An asymmetrically wide hump of the 0.47 mmol/g clay sample (1.52 nm) can be regarded as a composite of two different d_{001} values as shown in Figure 7b. The 00*l* reflection patterns with increasing amount of organic cations added are characteristic, and changes in the d_{001} values are given in Figure 8. The interlayer separation relative to basal spacing is defined here as Δ (nm) = $d_{001}-0.98$. The Δ value of the 0.23 mmol/g clay is 0.44 nm, and corresponds to the simple monolayer of the hydrocarbon chain lying in the interlayer space of the organoclay. The 1.62 nm d_{001} value (*i.e*. Δ = 0.64 nm) observed in Figure 7b for the 0.47 mmol/g clay is presumed to correspond to the arrangement of the semi-bilayer next to the basal plane in which adjacent alkyl tails partially overlap. Alternatively, a 1.62 nm *d* value would be more likely to be due to an interstratification of mono- and bi-layer configurations.

Referencing the d_{001} values and very broad 00*l* reflection profiles for the region 0.70−1.41 mmol/g clay, with increasing amounts of organic cations, the orderly arrangement of the organic cation molecules in the interlayer space is difficult to explain. It is more reasonable to envision disordered arrangements consisting of multiple configurations of the organic cations in the interlayer space, wherein the chain zigzag plane is parallel and/or perpendicular to the silicate layer (the van der Waals diameters are ~0.4 and 0.5 nm, respectively (Jordan, 1961)). Both these arrangements may exist simultaneously, especially in partially overlapping bilayers or paraffin-like structures at greater organic cation coverage.

In contrast, the 5 nm d_{001} value, and sharp reflections of higher-order 002, 003, 004, *etc.*, indicate that a high degree of order within the interlayer occurs in the organoclay complexes formed by addition of

https://doi.org/10.1346/CCMN.2008.0560105 Published online by Cambridge University Press

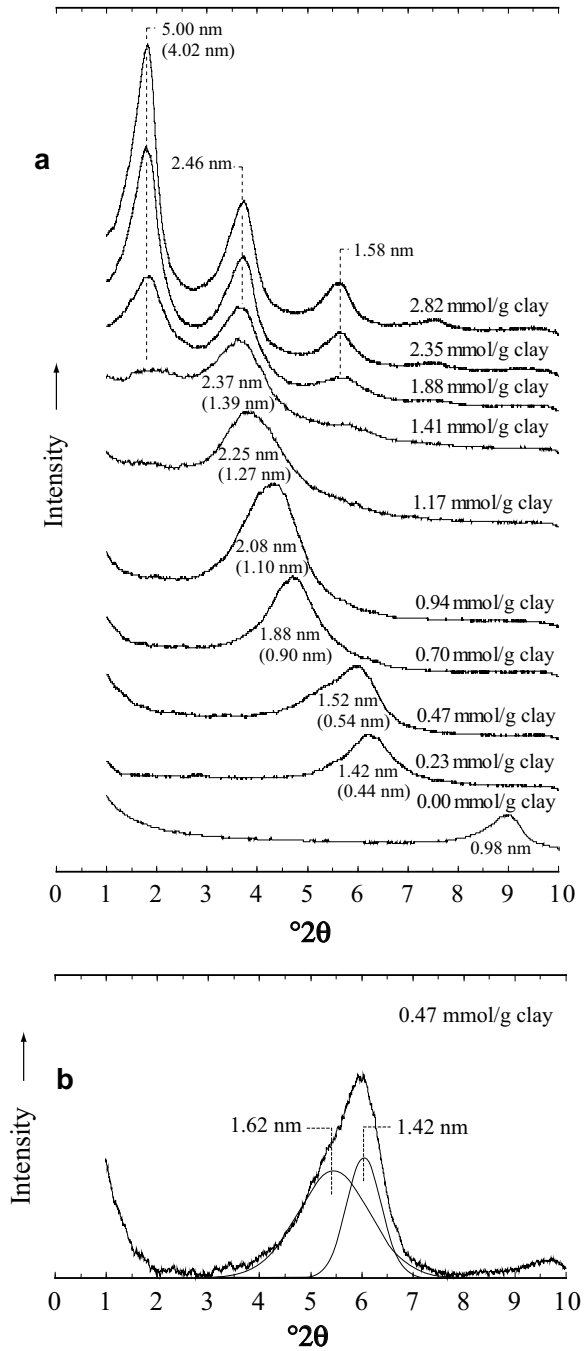

Figure 7. (a) Raw data of the XRD pattern of the basal plane of montmorillonite due to addition of TMDCA-Cl. As a reference, the 001 spacing of the initial montmorillonite at 0.98 nm was used here, and the increased distance of the lattice layers (*i.e.* $\Delta = d_{001} - 0.98$) is shown in parentheses under each d_{001} value. (b) Broad 001 peak of the 0.47 mmol/g clay is probably a composite of two peaks produced by having different d_{001} values (1.62 nm and 1.42 nm obtained with optimization of the non-linear least-squares method).

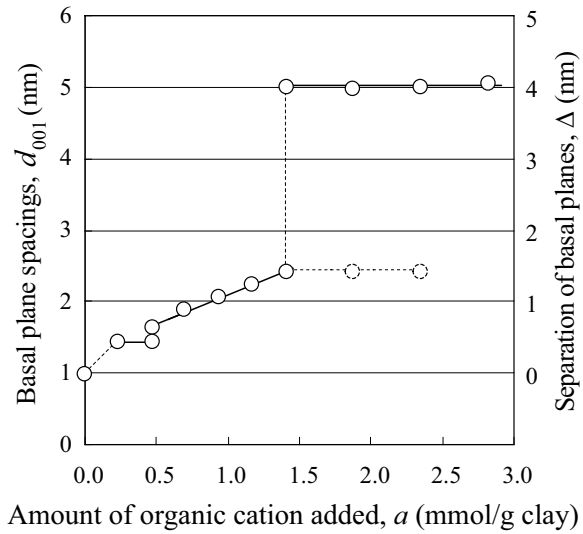

Figure 8. Plot of basal plane spacing *vs*. amount of organic cation added. Note: the standard d_{001} value of montmorillonite at 0.98 nm is plotted here.

>1.88 mmol TMDCA per g clay (>2.0 CEC). This can be interpreted as the alkyl chains of the organic cations being arranged with high order in a paraffin-like bilayer structure with their chain axis rising at a steep angle with respect to the silicate layers in the interlayer spaces of these organoclay complexes. A weak and very broad d_{001} hump of 5 nm is also observed in the 00*l* reflection trace for the 1.41 mmol/g clay.

When comparing the intensity ratios for the 001/002 reflections, the sample loading of 2.82 mmol/g clay shows a ratio of ~2:1, in which the 001 reflection is very sharp and of high intensity. However, the intensities of the 001 reflections for 2.35, 1.88, and 1.41 mmol/g clay are obviously less with decreased organic cation content, and the concurrent loss of intensity of the 002 reflections tends to be relatively small. This suggests that the interlayer structure is dominated by pseudotrimolecular layers, with the hydrocarbon chains parallel to the silicate surface. As illustrated in Figure 12, these structures may coexist with the paraffin-like arrangement in the silicate interlayers.

By monitoring with FTIR spectroscopy the frequency shifts of the CH_2 antisymmetric (ν_{as} CH_2) and symmetric (ν_s CH_2) stretching modes, the intercalated alkyl chains were found in states with varying degrees of conformational order. When the chains are highly ordered (all-*trans* zigzag conformation), the absorption bands appear around 2918 cm^{-1} (ν_{as} CH_2), and 2850 cm^{-1} (ν_s CH_2). On the other hand, if conformational disorder is included in the chains, their frequencies shift upwards, depending on the average content of *gauche* conformers (Vaia *et al*., 1994; Li and Ishida, 2003).

As seen in Figure 9a,b, appreciable shifts to the lower-frequency regions in the FTIR absorption spectra due to ν_s CH_2 at ~2850 cm^{-1} and ν_{as} CH_2 at ~2925 cm^{-1}

https://doi.org/10.1346/CCMN.2008.0560105 Published online by Cambridge University Press

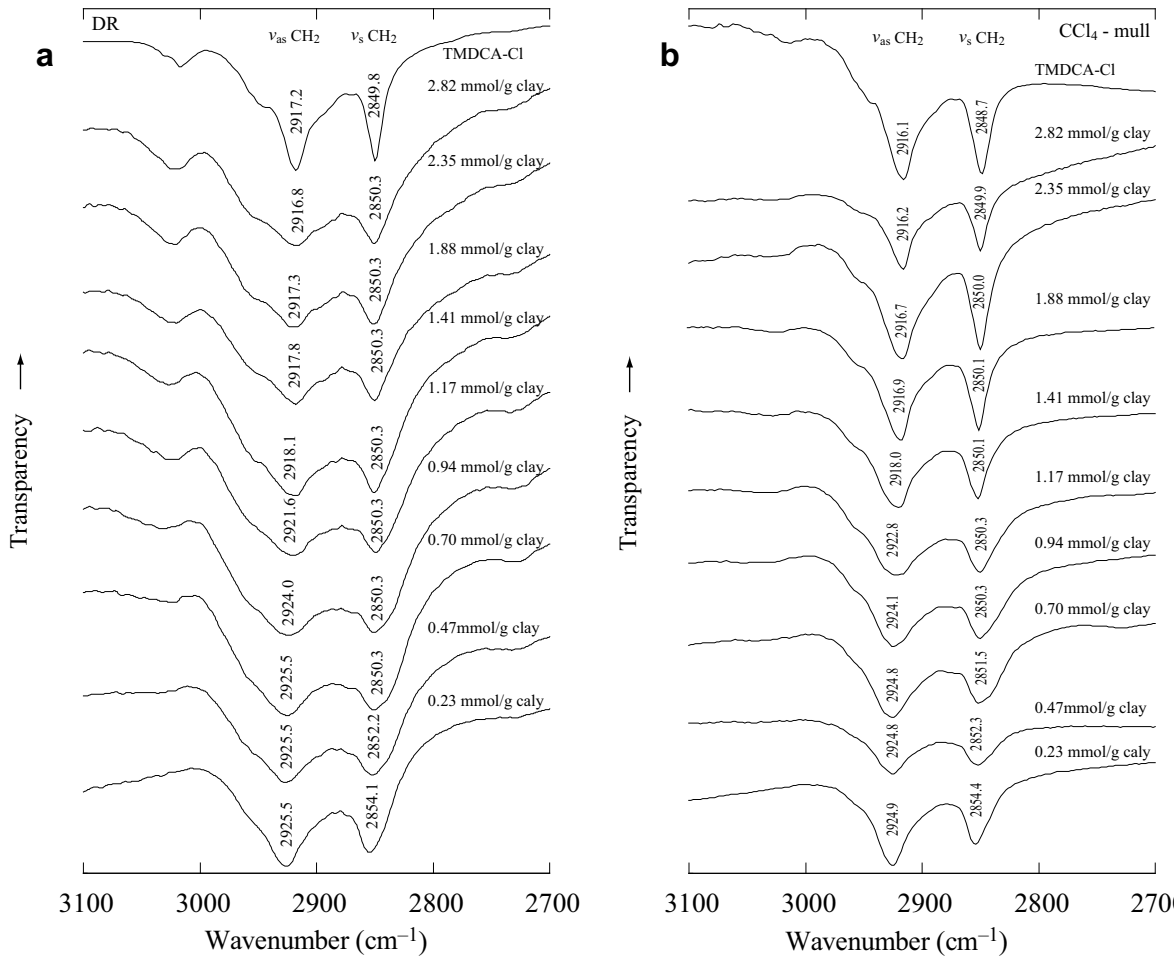

Figure 9. (a) CH_2-stretching vibrations in FTIR absorption spectra of TMDCA-Mt complexes (DR method). (b) CH_2-stretching vibrations in FTIR absorption spectra of TMDCA-Mt complexes (CCl_4-mull method).

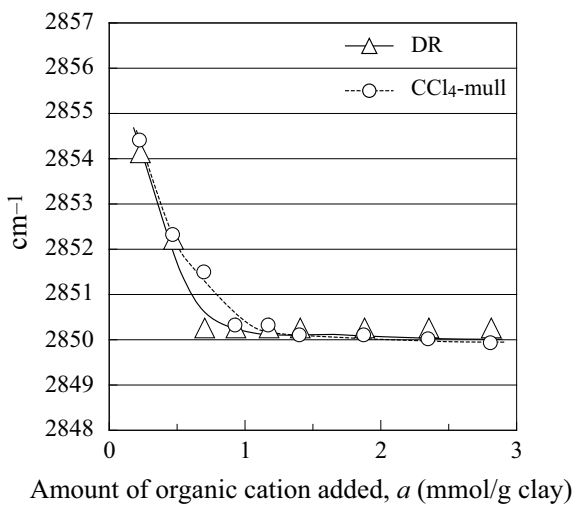

Figure 10. Change in the CH_2 symmetric stretching vibration *vs.* the amount of organic cation added.

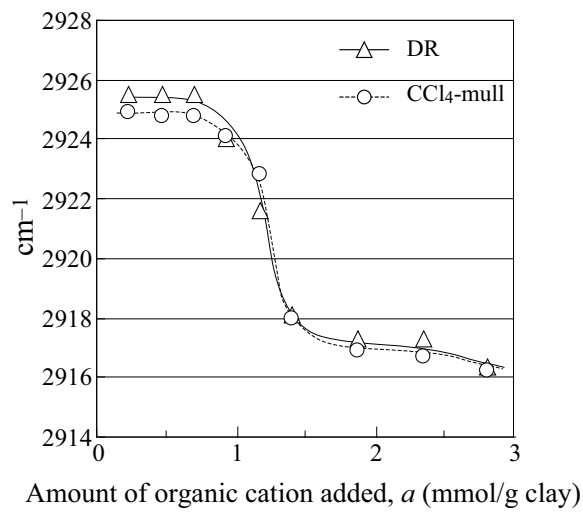

Figure 11. Change in CH_2 antisymmetric stretching vibration *vs.* the amount of organic cation added.

https://doi.org/10.1346/CCMN.2008.0560105 Published online by Cambridge University Press

were observed with increased numbers of organic cations added to the clay. The frequencies due to ν_s CH_2 (near 2850 cm^{-1}) and ν_{as} CH_2 (near 2925 cm^{-1}) are plotted as functions of the quantities of organic cation added to the clay in Figures 10 and 11, respectively, for all of the organoclay samples produced in the present study. Figure 10 shows that a large shift in the ν_s CH_2 frequency to the lower-frequency side occurs between 0.23 mmol/g clay and 0.94 mmol/g clay, and the frequency of the 0.94 mmol/g clay and beyond are followed by a relatively constant frequency, which equals that of the organic cation alone. Further, in Figure 11, the frequencies due to ν_{as} CH_2 are relatively constant between 0.23 mmol/g clay and 0.70 mmol/g clay. As additional organic cations are added to the clay between 0.94 mmol/g clay and 1.41 mmol/g clay, a large shift towards the lower-frequency side occurs and approaches the frequency of the organic cation alone. The inflection point of this shift corresponds to 1.41 mmol/g clay and, as shown in XRD patterns of Figure 8, it also corresponds to the point where the 5 nm structure of the d_{001} value begins to occur. From these findings, beyond the region of the amount of the stoichiometric equivalent of the organic cations (*i.e.* 0.94 mmol/g clay) to the CEC of the clay (*i.e.* 0.94 meq/ g clay), the evidence indicates that interactions between the adjacent hydrocarbon chains become progressively stronger due to van der Waals attraction.

However, it should be emphasized that FTIR data in Figures 9a,b, 10, and 11 tend to show that the coverage of ~0.70 mmol/g clay (1.88 nm intercalate) is paraffin-like in nature, as the CH_2 symmetric stretching is unchanged above that coverage. The inflection point in Figure 10 corresponds to sufficient formation of paraffin-like configuration. The changes in antisymmetric stretching (Figure 11) occur where considerable disorder exists — between 0.70 and 1.41 mmol/g clay — in the paraffin-like configuration. It becomes highly ordered above 1.41 mmol/g clay where initiation of the 5 nm d_{001} peak in the 1.41 mmol/g clay occurs (Figure 7a).

The half-width of the observed d_{001} reflection is well known to depend on variations in layer stacking order-disorder in the *c*-axis direction, and disorders commonly arise from the presence of variable amounts of intercalated material between the layers. Here, half widths of the 001 reflections of TMDCA-Mt complexes of 0.70 mmol/g clay or more, where the hydrocarbon chains of the organic cation molecules arrange as bilayer parallel to the basal planes of the clay, were plotted in Figure 13 as a function of the amount of organic cations added to the clay. Maximum half widths were obtained in the region 0.94–1.17 mmol/g clay, and the half widths for the various organoclays decreased rapidly as the amount of the organic cations added to the clay diverged from this region, corresponding to an ammonium *vs.* clay ratio of 1.00–1.25 CEC. Ordered and/or disordered arrangements of the organic cations intercalated between the layers may be responsible for the half widths.

Van Olphen (1963) gave the total layer surface area of 750 m^2/g clay for a model Na-montmorillonite, $(Si_8)(Al_{10/3}Mg_{2/3})O_{20}(OH)_4 \cdot Na_{2/3}$ (FW = 734), having a cell surface area of $5.15 \times 8.9 \times 10^{-20} = 45.8$ m^2 on each side. Values of 46.5×10^{-20} m^2/a_0b_0 and 49×10^{-20} m^2/a_0b_0, respectively, for dioctahedral and trioctahedral layer silicate were used by Lagaly and Weiss (1969) and Lagaly *et al.* (1976). Poor agreement is, thus, found among cell areas and $d_{100}d_{010}$ values reported for dioctahedral layer silicates. Instead of using the ideal total layer surface area mentioned above, for the purposes of this study the total layer surface area of the initial clay is defined as 625 m^2/g, based on the CEC value (0.94 mmol/g) and the projected area of methylene blue molecule (55.25×10^{-20} m^2, Huang and Brindley, 1970). For the TMDCA cation, when the C-C zigzag is lying parallel to the layer silicate surface, the projected area will be accepted as 165×10^{-20} m^2/ion (= 3.30 nm × 0.5 nm). For perpendicular orientation of the C-C zigzag plane, the accepted value is 132×10^{-20} m^2/ion (= 3.30 nm × 0.4 nm). At organic cation loadings above 0.31 mmol/g, the monolayer coverage changes to bilayer coverage, which itself is present until coverage exceeds 0.62 mmol/g clay. Thus, for any coverage above 30% of the CEC, the interlayer configuration must be at least bilayer, and coverage >~65% must be pseudotrimolecular or paraffin-like in configuration. Interstratifications of all these configurations undoubtedly occur. Coverage as high as 100% of the CEC would require three times the interlayer surface that is available for flat-lying organic cations. Of course above the 100% CEC coverage, the size and influence of the anion (chloride) must also be taken into consideration (Slade and Gates, 2004a, 2004b), and thus some dispersion in the reflections is observed.

If a paraffin-like arrangement takes place, the angle of rise between the C-C zigzag plane and the silicate surface would increase linearly with increasing surface coverage. This is observed for the 0.7 to 1.17 mmol/g clay coverage. The 5 nm *d* value observed for the greatest loadings probably corresponds to a paraffin-like bilayer arrangement, with the alkyl tails in *trans* conformations rising at least 37° from the surface of the clay, according to $\sin^{-1}[(5-0.98)/(2 \times 3.30)]$. Assuming that an overlap of ~8 carbon atoms occurs (corresponding to ~1.07 nm) for alkyl tails arising from opposing surfaces, the angle of rise is ~47° (= $\sin^{-1}[(5-0.98)/(2 \times 3.30-1.07)]$). This amount of overlap would give rigidity to the intercalate complex and provide room for the anions to alternate within the center of the interlayer space. Greater overlap will only give a larger angle of rise if the d_{001} values decrease (Slade and Gates, 2004a, 2004b). However, as no

https://doi.org/10.1346/CCMN.2008.0560105 Published online by Cambridge University Press

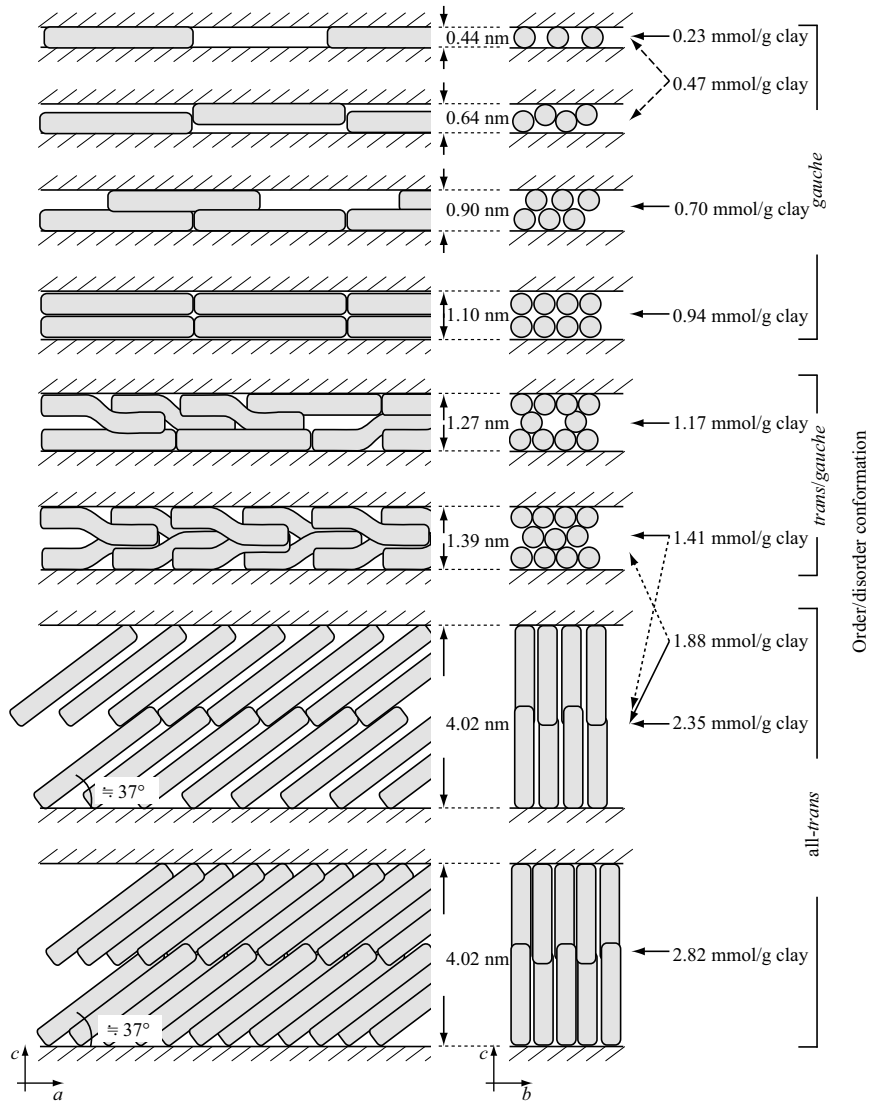

Figure 12. Schematics for alkyl-chain aggregation in the montmorillonite interlayer *vs*. the amount of organic cation added.

experimental evidence for the overlap was observed in this study, we assume a paraffin-like bilayer arrangement having a 37º angle of rise as illustrated in Figure 12.

Furthermore, it is considered that a larger diameter of the head group than width of the tail in the TMDCA cation creates some spatial freedom between the adjacent chains and consequently may contribute to conformational disorder of the C-C zigzag chains. Such disorder within the interlayer space as a function of organocation loading may be reflected in the larger half widths of 001 reflections for the various arrangements, orientations, and conformations. Schematics for the various aggregations of the alkyl chain in the interlayers according to the amount of organic cations presumed from these results are shown in Figure 12.

The relationship between the structure and the organophilic characteristics of TMDCA-Mt complexes

The relative sediment volume, S', from the NPO suspensions and the specific gel volume of toluene, f_t, were subsequently plotted as a function of the organic cation loadings in Figure 13. The half width data of the 001 reflection were also plotted for comparison with S' and f_t in Figure 13. The values of S' and f_t increased as the half width increased, and each maximum region had a similar location on the abscissa of the organic cation loadings. This means that TMDCA-Mt complexes, with large half widths, have large swelling capacities in non-polar organic solvents such as toluene and NPO.

Figure 14 shows XRD patterns on four pre-gel specimens consisting of NPO and TMDCA-Mt complexes (7 wt.%) mentioned earlier. The XRD patterns of

https://doi.org/10.1346/CCMN.2008.0560105 Published online by Cambridge University Press

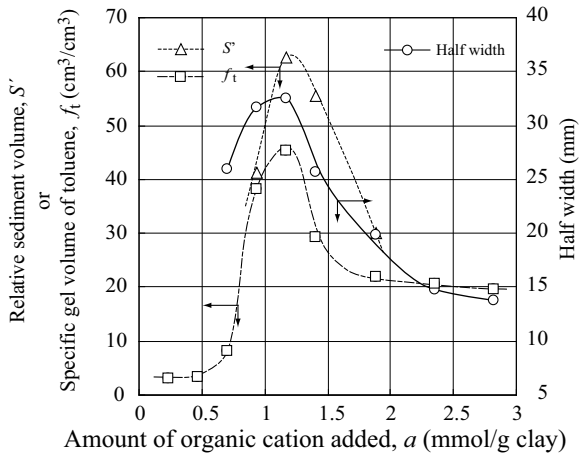

Figure 13. Changes of relative sediment volume, S', in NPO suspensions, specific gel volume of toluene, f_t, and the half width of the 001 reflection by XRD, *vs.* the amount of organic cation added.

both pre-gel specimens, containing TMDCA-Mt complexes of 0.94 and 1.17 mmol/g clay, respectively, have the largest half widths for the 001 reflections, and are typical gel patterns because no detectable reflections from montmorillonite lattices are present. The XRD patterns of the pre-gel specimens, containing 1.41 and 1.88 mmol/g clay complexes, respectively, exhibit integral 001-series reflections due to the montmorillonite lattices, resulting from rearrangement of the long alkyl chains intercalated between the silicate layers, developed by mixing during the pre-gel preparation process. Therefore, though the d_{001} value of the organoclay particles is a large value beyond 5 nm, it still belongs to the category of crystalline swelling of the organoclay. This demonstrates that these organoclays have poor swelling and solvation capacities for the NPO

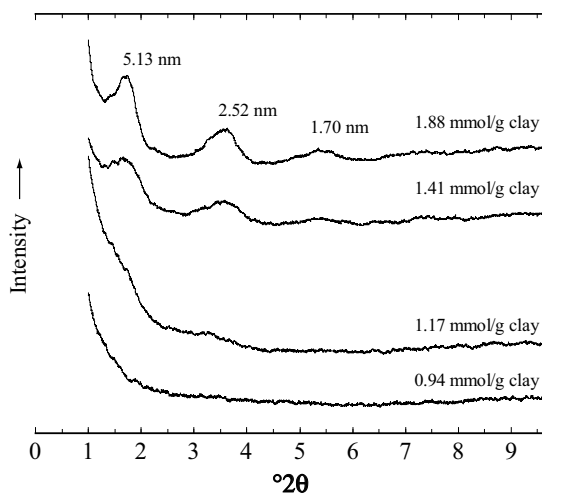

Figure 14. XRD patterns of the pre-gel prepared by mixing TMDCA-Mt and NPO.

medium, because the van der Waals attractions between close-packed, long and massive alkyl chains themselves develop crystallization of the hydrocarbon chains and form an exclusive structure from external non-polar organic solvents in the interlayer space of the clay, resulting in inhibition of solvation with organic solvents.

In contrast, the TMDCA-Mt complexes, where the intercalates cover the silicate surfaces but are irregularly distributed and the alkyl tails are randomly arranged or disordered, *e.g.* the 0.94 and 1.17 mmol/g clay loadings, form a more open structure for external organic liquids. Once the organic liquid solvates the organoclay complex, it greatly weakens the van der Waals forces acting between the alkyl chains, and perhaps van der Waals interaction between the organic liquid and the alkyl chains leads to greater disorder in the interlayer structure, due to macroscopic swelling, *via* solvation.

This would be supported by a theory developed by Slade and Gates (2004a, 2004b) who suggested that toluene, with its capacity to weaken the van der Waals forces between close-packed hydrocarbon chains of hexadecyltrimethylammonium clay, and possibly bind to them directly *via* these forces, leads to disordering of the interlayer structure. A similar intercalate structure in smectites was implied for benzyloctadecyldimethylammonium smectites upon sorption of ethanol (Gates, 2004).

CONCLUSIONS

Organophilic bentonite was prepared by reacting natural Na-montmorillonite with trimethyldococylammonium chloride having a long *n*-alkyl of 22 carbon atoms. The viscosity of the non-polar organic liquid suspensions of these organoclay complexes was measured and the organoclay particle morphology in the suspensions was investigated according to Eyring's rate process and Robinson's relative sediment volume. The organoclay products prepared by adding the organic cations at ratios of 0.94 and 1.17 mmol/g clay, exhibited the greatest number of relative sediment volume and of specific gel volume of toluene. The former is considered dynamic swelling capacity and the latter is static.

The results from the stoichiometry of the organoclay complex formation investigated using DTGA, and from the structural analyses of the organoclay complexes using XRD and FTIR spectroscopy, showed that the silicate layer surface of the clay is well covered with hydrocarbon chains and has a disordered structure of organic cations in the interlayer space of the clay, contributing to a more organophilic nature by promoting solvation of the organoclay complexes by external non-polar organic liquids. However, the interaction between the long and massive dococyl chains themselves brings a tendency that develops crystallization of the organic cations existing in the interlayer. Although the basal spacing would be increased to as much as 5 nm, these

https://doi.org/10.1346/CCMN.2008.0560105 Published online by Cambridge University Press

crystalline swelling structures persisted, resulting in inhibition of solvation by external non-polar organic liquids.

We discovered that the relative magnitude of half width of the 001 reflection is consistent with the disordering of the interlayer structure affecting organophilicity.

REFERENCES

Bingham, E. (1922) *Fluidity & Plasticity*. McGraw-Hill Co. Berkshire, UK, 440 pp.

Bish, D.L. and Duffy, C.J. (1990) Thermogravimetric analysis of minerals. Pp. 127–129 in: *Thermal Analysis in Clay Science* (J.W. Stucki, D.L. Bish, and F.A. Mumpton, editors). CMS Workshop Lectures **3**, The Clay Minerals Society, Boulder, Colorado.

Bonczek, J.L., Harris, W.G., and Nkedi-Kizza, P. (2002) Monolayer to bilayer transitional arrangements of hexadecyltrimethylammonium cations on Na-montmorillonite. *Clays and Clay Minerals*, **50**, 11–17.

Brindley, G.W. and Lemaitre, J. (1987) Thermal, oxidation and reduction reactions of clay minerals. Pp. 321 in: *Chemistry of Clays and Clay Minerals* (A.C.D. Newman, editor). Monograph **6**, Mineralogical Society, London.

Brown, G., editor (1961) *The X-ray Identification and Crystal Structure of Clay Minerals*. P. 181, Mineralogical Society, London.

Egashira, K. (1977) Viscosities of allophane and imogolite clay suspensions. *Clay Science*, **5**, 87–95.

Einstein, A. (1906) Eine neue Bestimmung der Molekuldimension. *Annalen der Physik*, **19**, 289–306.

El-Akkada, T.M., Flex, N.S., Guindy, N.M., El-Massry, S.R., and Nashed, S. (1982) Thermal analyses of mono- and divalent montmorillonite cationic derivatives. *Thermochimica Acta*, **59**, 9–17**.**

Gabrysh, W.F., Eyring, H., Lin-Sen, P., and Gabrysh, A.F. (1963) Rheological factors for bentonite suspensions. *Journal of the American Ceramic Society*, **46**, 523–529.

Gates, W.P. (2004) Crystalline swelling of organo-modified clays in ethanol-water solutions. *Applied Clay Science*, **27**, 1–12.

Green, H. (1949) *Industrial Rheology and Rheological Structures*. P. 127, J. Wiley & Sons, New York.

Grim, R.E. (1962) *Applied Clay Mineralogy*. Pp. 205–216. McGraw-Hill, New York.

Grim, R.E. (1968) *Clay Mineralogy*. Pp. 313–328 McGraw-Hill, New York.

Güven, N. (1992a) Rheological aspects of aqueous smectite suspensions. Pp. 82–88 in: *Clay-Water Interface and its Rheological Implications* (N. Güven and R.M. Pollastro, editors). CMS Workshop Lectures, **4**, The Clay Minerals Society, Boulder, Colorado.

Güven, N. (1992b) *Rheological aspects of aqueous smectite suspensions*. Pp. 90–92 in: *Clay-Water Interface and its Rheological Implications* (N. Güven and R.M. Pollastro, editors). CMS Workshop Lectures, **4**, The Clay Minerals Society, Boulder, Colorado.

Hauser, E.A. (1950) Modified gel-forming clay and process of producing same. U.S. Patent, 2,531,427, Nov. 28 (1950).

He, H., Frost, R.L., Deng, F., Zhu, J., Wen, X., and Yuan, P. (2004) Conformation of surfactant molecules in the interlayer of montmorillonite studied by ^{13}C MAS NMR. *Clays and Clay Minerals*, **52**, 350–356.

Huang, P.M. and Brindley, G.W. (1970) Methylene blue absorption by clay minerals. Determination of surface areas and cation exchange capacities (clay-organic studies XVIII). *Clays and Clay Minerals*, **18**, 203–212.

Jordan, J.W. (1949) Organophilic bentonites. I. Swelling in organic liquids. *Journal of Physical and Colloid Chemistry*, **53**, 294–306.

Jordan, J.W. (1961) Organophilic clay-base thickeners. *Proceedings of the Tenth National Conference on Clays and Clay Minerals*. Pp. 299–308.

Jordan, J.W., Hook, B.J., and Finlayson, C.M. (1950) Organophilic bentonites. II. Organic liquid gels. *Journal of Physical and Colloid Chemistry*, **54**, 1196–1208.

Kuhn, W. and Kuhn, H. (1945) Die abhangigkeit der viskositat vom stromungsgefalle bei hoch verdunnten suspensionen und lösungen. *Helvetica Chimica Acta*, **28**, 97–127.

Lagaly, G. and Weiss, A. (1969) Determination of the layer charge in mica-type silicates. *Proceedings of the International Clay Conference*, *1969*, *Tokyo*, **1**. Pp. 61–80. Israel Universities Press, Jerusalem.

Lagaly, G. and Weiss, A. (1970) Inhomogeneous charge distributions in mica-type layer silicates. *Proceedings of 'Reunion Hispano-Belga Minerales de la Arecilla'*. Pp. 179–187. Consejo Superior de Investigaciones Cientificos, Madrid.

Lagaly, G., Fernandez Gonzalez, M., and Weiss, A. (1976) Problems in layer-charge determination of montmorillonites. *Clay Minerals*, **11**, 173–187.

Lee, S.Y. and Kim, S.J. (2002) Expansion of smectite by hexadecyltrimethylammonium. *Clays and Clay Minerals*, **50**, 435–445.

Li, Y. and Ishida, H. (2003) Concentration-dependent conformation of alkyl tail in the nanoconfined space: Hexadecylamine in the silicate galleries. *Langmuir*, **19**, 2479–2484.

Low, P.F. (1992) Interparticle forces in clay suspensions: flocculation, viscous flow and swelling. Pp. 163-171 in: *Clay-Water Interface and its Rheological Implications* (N. Güven and R.M. Pollastro, editors). CMS Workshop Lectures, **4**, The Clay Minerals Society, Boulder, Colorado.

Mitchell, J.K. and Soga, K. (2005) *Fundamentals of Soil Behavior*. John Wiley & Sons, New Jersey, USA, pp. 95–97.

Minase, M., Kondo, M., Onikata, M., and Kawamura, K. (2006) The viscosity of suspensions of bentonite. *Clay Science*, **12**, Supplement **2**, 125–130. ICC 2005: *Clay sphere – Past, present and future*. *Proceedings of the 13^{ih} International Clay Conference Tokyo, Japan.*

Mori, Y. and Ototake, N. (1956) On the viscosity of suspensions. *Chemical Engineering, Japanese*, **9**, 488–494.

Onikata, M. and Kondo, M. (1995) Rheological properties of the partially hydrophobic montmorillonite treated with alkyltrialkoxysilane. *Clay Science*, **9**, 299–310.

Park, K., Ree, T., and Eyring, H. (1971) Effect of electrolytes on flow properties of aqueous bentonite suspension. *Journal of the Korean Chemical Society*, **15**, 303–312.

Powell, R.E. and Eyring, H. (1944) Mechanisms for the relaxation theory of viscosity. *Nature*, **154**, 427–428.

Robinson, J.V. (1949) The viscosity of suspensions of spheres. *Journal of Physical and Colloid Chemistry*, **53**, 1042–1056.

Slade, P.G. and Gates, W.P. (2004a) The swelling of HDTMA smectites as influenced by their preparation and layer charges. *Applied Clay Science*, **25**, 93–101.

Slade, P.G. and Gates, W.P. (2004b) The ordering of HDTMA in the interlayers of vermiculite and the influence of solvents. *Clays and Clay Minerals*, **52**, 204–210.

Suito, E., Arakawa, M., and Kondo, M. (1966a) Adsorbed state of organic compounds in organo-bentonite I. Infrared study. *The Bulletin of the Institute for Chemical Research, Kyoto University*, **44**, 316–324.

Suito, E., Arakawa, M., and Yoshida, T. (1966b) Adsorbed state of organic compounds in organo-bentonite II.

Differential thermal analysis. *The Bulletin of the Institute for Chemical Research, Kyoto University*, **44**, 325–334.

Suito, E., Arakawa, M., and Yoshida, T. (1969) Electron microscopic observation of the layer of organo-montmorillonite. *Proceedings of the International Clay Conference, 1969, Tokyo*, **1**, Pp. 757–763. Israel Universities Press, Jerusalem.

Suito, E. and Yoshida, T. (1971) Interstratified layer structure of the organo-montmorillonites as revealed by the electron microscopy. *Abstracts U.S.–Japan Seminar on Clay-Organic Complexes*, Pp. 53–62.

Vaia, R.A., Teukolsky, R.K., and Giannelis, E.P. (1994) Interlayer structure and molecular environment of alkylammonium layered silicates. *Chemistry of Materials*, **6**, 1017–1022.

Van Olphen, H. (1977) *An Introduction to Clay Colloid Chemistry*. Pp. 254–256, J. Wiley & Sons, New York.

(*Received 13 October 2006; revised 17 August 2007; Ms. 1226; A.E. Will P. Gates*)